ISSN 0915-633X

NATIONAL INSTITUTE FOR FUSION SCIENCE

Simulations of Toroidal Current Drive Without External Magnetic Helicity Injection

Y. Kondoh, M. Yamaguchi and K. Yokozuka

(Received - June 10, 1996)

NIFS-422 July 1996

RESEARCH REPORT
NIFS Series

NAGOYA, JAPAN

Simulations of toroidal current drive without external magnetic helicity injection

Y. Kondoh, M. Yamaguchi and K. Yokozuka

Dept. of Electronic Engineering, Gunma University, Kiryu, Gunma 376, Japan

Abstract

It is shown by three-dimensional magnetohydrodynamic simulations that the toroidal current J_z can be induced by a process of relaxation without helicity invariance under no external magnetic helicity injection. It is shown that the magnetic helicity is induced during relaxation and it is passively determined as a result of the time evolution of the dynamical system. Numerical results suggest that the basic process for the toroidal current drive during relaxation is the nonlinear energy transfer from the toroidal magnetic energy to the poloidal one under the intervention of the kinetic energy. It is demonstrated that the self-organization to the lower eigenmode with a larger scale structure occures during relaxation.

Keywords: relaxation, helicity, 3D simulation, MHD plasma, nonlinear, energy transfer, self-organization,

After the conjecture of the magnetic helicity invariant was successfully introduced by J. B. Taylor in his well-known relaxation theory for the interpretation of the self-organized reversed field pinch (RFP) configuration [1, 2], "the magnetic helicity" has been used for "the current drive experiment by helicity injection". Although the magnetic helicity is only a measure for linkage and knotting of the flux tubes in order to describe the topology of the magnetic fields in plasmas [3, 4], it has been treated as if it were a sort of real physical quantity. When we assume the Ohm's law of $\eta\,\mathbf{j} = \mathbf{E} + \mathbf{v} \times \mathbf{B}$, the transport equation (the conservation law) of the magnetic helicity [1, 2, 4] is given by

$$\frac{\partial K_m}{\partial t} = -2 \int \eta\,\mathbf{j} \cdot \mathbf{B} \mathrm{d}V - \oint (\mathbf{E} \times \mathbf{A} + \phi \mathbf{B}) \cdot \mathrm{d}\mathbf{S}\,. \tag{1}$$

Here, the surface integral term of $\oint (\mathbf{E} \times \mathbf{A} + \phi \mathbf{B}) \cdot \mathrm{d}\mathbf{S}$ is used for the experiments of the current drive by helicity injection, and it becomes zero when the boundary surface is the ideally conducting wall. The term of $\int \eta\,\mathbf{j} \cdot \mathbf{B} \mathrm{d}V$ has been explained as a loss term of helicity due to the resistivity η [1, 2]. However, this is not correct, because it becomes an induction term as well as the loss term, depending on the relative direction between $\mathbf{j}$ and $\mathbf{B}$. On the other hand, the self-organization theory based on autocorrelations [5, 6] suggests a possibility of current drive in self-organizing plasmas independent of the magnetic helicity invariant. In order to clarify that the magnetic helicity is induced by the term of $\int \eta\ \mathbf{j} \cdot \mathbf{B} \mathrm{d}V$ and it is passively determined as a result of the time evolution of dynamical systems, we carried out three-dimensional (3-D) simulations for "the current drive without magnetic helicity injection" by using a magnetohydrodynamic (MHD) code under the boudary condition of the ideally conducting wall. The simulation model used here is a compressible, zero-β ($\nabla p = \mathbf{0}$), disspative MHD plasmas without viscousity described by the following equations [7]

$$\frac{\partial \rho}{\partial t} = -\nabla \cdot (\rho \mathbf{u})\,, \tag{2}$$

$$\frac{\partial \rho \mathbf{u}}{\partial t} = -\nabla \cdot (\rho \mathbf{u}\mathbf{u}) + \mathbf{j} \times \mathbf{B} . \tag{3}$$

$$\frac{\partial \mathbf{B}}{\partial t} = \nabla \times (\mathbf{u} \times \mathbf{B}) - \nabla \times (\eta \mathbf{j}) , \tag{4}$$

$$\mathbf{j} = \frac{1}{\mu_0} \nabla \times \mathbf{B} . \tag{5}$$

The explicit and second order Richtmyer method is used for the difference scheme in our 3-D MHD simulation code. Simulation domain is a rectangular column which is implemented on a $(41 \times 41 \times 82)$ point grid and is periodic along z axis (the toroidal direction) with a periodic length L and enclosed by perfectly conducting wall at $x = y = \pm a$. Normalization method of variables and boundary conditions are all the same as those in [8]. We used here a fixed nonuniform resistivity profile given by $\eta = \eta_c \{ 1.0 + 19.5[(x/a)^8 + (y/a)^8]\}$, where η_c is the value of η at the center of $x = y = 0$. Numerical results for the magnetic Reynolds number of $R_\eta = \mu_0 a v_A / \eta_c = 10^5$ are shown here, where v_A is the initial value of the mean Alfvén velocity, and the time t is measured by the Alfvén time t_A defined by $t_A = a/v_A$.

As an initial condition, we adopt a simple distribution of toroidal magnetic fields given by $B_z = B_0 \cos\pi(y+a)/2a + B_{z0}$ with values of $B_0 = 4000$ and $B_{z0} = 4.0$. The first component of the toroidal fields B_z corresponds to the toroidal field produced by an initial external current j_x. This initial distribution of magnetic fields has no magnetic helicity because of no linkage of the flux tubes. Initial plasma density is assumed to be spatially uniform, and initial velosity is given by $u_z = 0.06 \cos\pi(x + a)/2a$. Perturbation fields of high mode components and force-free fields with small amplitudes (less than 1/200 of the initial toroidal fields) are superposed on the initial distribution of magnetic fields.

Figure 1 shows the temporal evolutions of the normalized parallel component $J_\parallel$ (solid line) and perpendicular component $J_\perp$ (dashed line) of the electric current

obtained from the simulation. Here, the normalized components $J_{\|}$ and $J_{\perp}$ are defined respectively by $J_{\|} = <| \mathbf{j}_{\|} | / | \mathbf{j} |>$ and $J_{\perp} = <| \mathbf{j}_{\perp} | / | \mathbf{j} |>$, where $\mathbf{j}_{\|} = (\mathbf{j} \cdot \mathbf{B})\mathbf{B}/(\mathbf{B} \cdot \mathbf{B})$, $\mathbf{j}_{\perp} = \mathbf{j} - \mathbf{j}_{\|}$, and $< F >$ denotes the volume average. The initial current density are almost perpendicular to the magnetic field. The parallel component $J_{\|}$ increases rapidly and reaches the high amplitude comparable to the perpendicular component $J_{\perp}$.

In the present simulation, the initial magnetic helicity is almost zero and there is no helicity injection through the ideally conducting boundary wall. Therefore, using the induced parallel component $\mathbf{j}_{\|}$ and integrating Eq.(1) over time, we can evaluate the magnetic helicity. Figure 2 shows the temporal evolution of the magnetic helicity obtained from the simulation. The magnetic helicity is shown to be induced and increase rapidly during relaxation.

Figure 3 shows the temporal evolutions of the toroidal (dashed line) and the poloidal (solid line) magnetic energies. We see that some part of the toroidal magnetic energy is transfered to the poloidal magnetic energy during relaxation.

Since the change rate of magnetic helicity normalized by the initial helicity becomes quite large compared with that of magnetic energy, Taylor's conjecture on the magnetic helicity invariant during relaxation [1, 2] is not realized in the present simulation of relaxation.

Figure 4 shows the temporal evolutions of the averaged toroidal currents, where $\int J_z \mathrm{d}V/V$ and $\int J_z \mathrm{d}S/S$ denote the averaged value over the volume and that over a x-y cross section, respectively. We see from Fig. 3 that although there is no magnetic helicity injection, the toroidal current J_z is acturally induced by the process of relaxation without helicity invariance.

Figure 5 shows the temporal evolution of the total magnetic energy W_m and the total kinetic energy W_k, both of which are normalized by the initial magnetic energy

W_{m0}. The phase of increase of kinetic energy coincides with the phase of the higher decrease of the magnetic energy. When the kinetic energy decreases, the decay rate of magnetic energy becomes lower. This result indicates that the kinetic energy and the magnetic energy interchanges with each other during relaxation. Comparison of Figs. 3 and 5 suggests that the toroidal magnetic energy is nonlinearly transfered to the poloidal magnetic energy under the intervention of the kinetic energy.

Figure 6 shows the profile of the poloidal magnetic field (B_x, B_y) at $t = 10\, t_A$. We see that the self-organization [5, 6, 9, 10] to the lower eigenmode with a larger scale structure occurs during the present relaxation.

In conclusion, we have demonstrated by 3-D MHD simulations that the toroidal current J_z can be induced by a process of relaxation without helicity invariance under no external magnetic helicity injection. We have shown that the magnetic helicity is induced during relaxation by the term of $\int \eta\, \mathbf{j} \cdot \mathbf{B} dV$ for the case with no initial magnetic helicity and it is passively determined as a result of the time evolution of the dynamical system. Comparison of Figs.3 and 5 suggests that the basic process for the toroidal current drive during relaxation is the nonlinear energy transfer from the toroidal magnetic energy to the poloidal one under the intervention of the kinetic energy. It has been demonstrated that the self-organization to the lower eigenmode with a larger scale structure occures during relaxation.

The authors wish to acknowledge valuable discussion and comments on this work by Professors T. Sato and T. Hayashi at the National Institute for Fusion Science. This work was carried out under the collaborative research program at the National Institute for Fusion Science, Nagoya, Japan.

REFERENCES

[1] J. B. Taylor: Phys. Rev. Lett. **33**, 1139 (1974).

[2] J. B. Taylor: Rev. Mod. Phys. **58**, 741 (1986).

[3] H. K. Moffatt, *Magnetic Field Generation in Electrically Conducting Fluids* (Cambridge Univ. Press, Cambridge, England, 1978).

[4] R. L. Stenzel, J. M. Urrutia, and C. L. Rousculp: Phys. Rev. Lett. **74**, 702 (1995).

[5] Y. Kondoh: Phys. Rev. E **48**, 2975 (1993).

[6] Y. Kondoh: Phys. Rev. E **49**, 5546 (1994).

[7] Y. Kondoh, Y. Hosaka, J. Liang, R. Horiuchi and T. Sato: J. Phys. Soc. Jpn. **63**, 546 (1994).

[8] R. Horiuchi and T. Sato: Phys. Fluids **29**, 4174 (1986).

[9] Y. Kondoh and J. W. Van Dam: Phys. Rev. E **52**, 1721 (1995).

[10] Y. Kondoh, T. Yumoto, M. Yamaguchi, N. Kondo, R. Horiuchi and T. Sato: J. Plasma and Fusion Res. **71**, 432 (1995).

Figure captions

Fig.1. Temporal evolutions of the normalized parallel component $J_{\parallel}$ (solid line) and perpendicular component $J_{\perp}$ (dashed line) of the electric current.

Fig.2. Temporal evolution of the magnetic helicity.

Fig.3. Temporal evolutions of the toroidal (dashed line) and the poloidal (solid line) magnetic energies.

Fig.4. Temporal evolutions of the averaged toroidal currents, where $\int J_z \mathrm{d}V/V$ and $\int J_z \mathrm{d}S/S$ denote the averaged value over the volume and that over a x-y cross section, respectively.

Fig.5. Temporal evolution of the total magnetic energy W_m and the total kinetic energy W_k, both of which are normalized by the initial magnetic energy W_{m0}.

Fig.6. The profile of the poloidal magnetic field (B_x, B_y) on a x-y cross section at $t = 10\ t_A$.

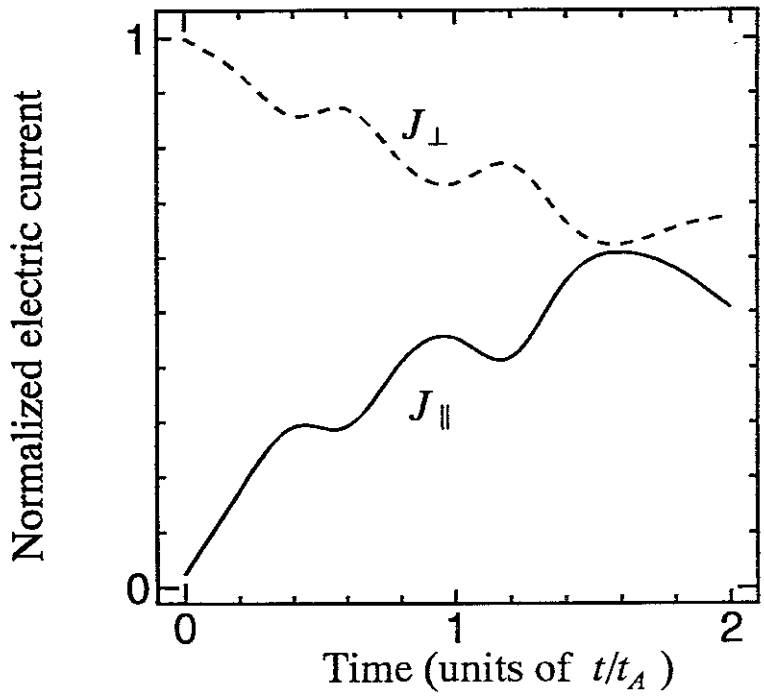
Normalized electric current
1
0
$J_\perp$
$J_\parallel$
0
1
2
Time (units of t/t_A)

Fig.1

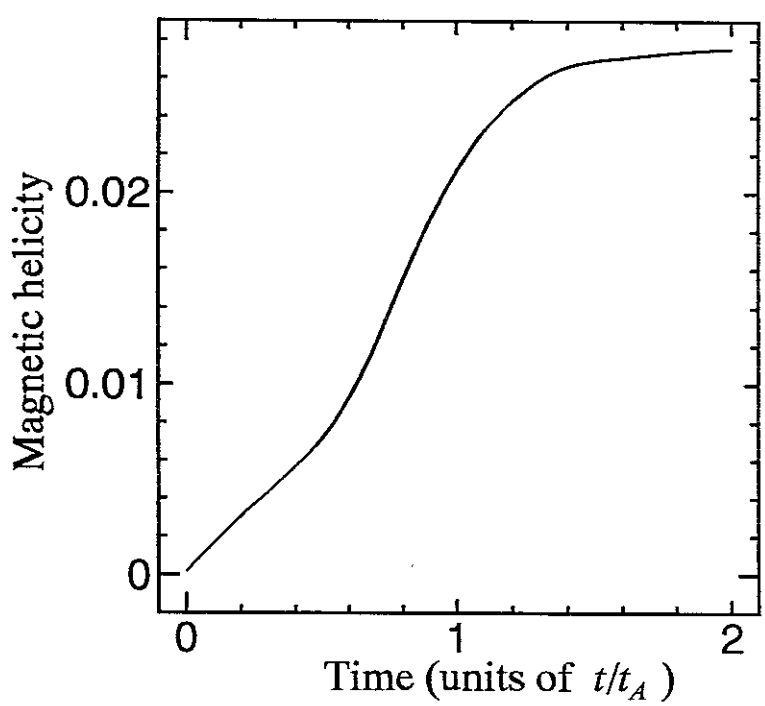
Magnetic helicity
0.02
0.01
0
0
1
2
Time (units of t/t_A)

Fig.2

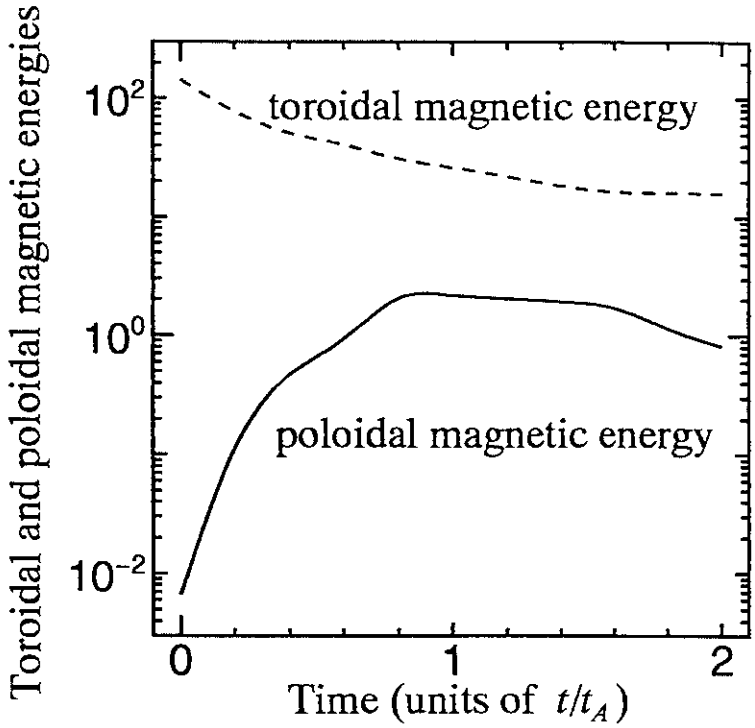
Toroidal and poloidal magnetic energies
10^2
10^0
10^{-2}
toroidal magnetic energy
poloidal magnetic energy
0
1
2
Time (units of t/t_A)

Fig.3

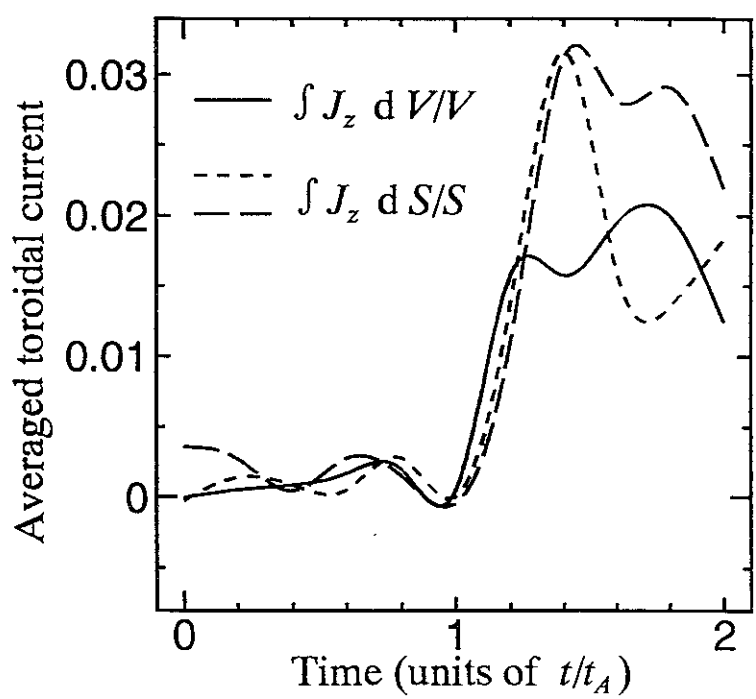
Averaged toroidal current
0.03
0.02
0.01
0
$\int J_z \, \mathrm{d}\, V/V$
$\int J_z \, \mathrm{d}\, S/S$
0
1
2
Time (units of t/t_A)

Fig.4

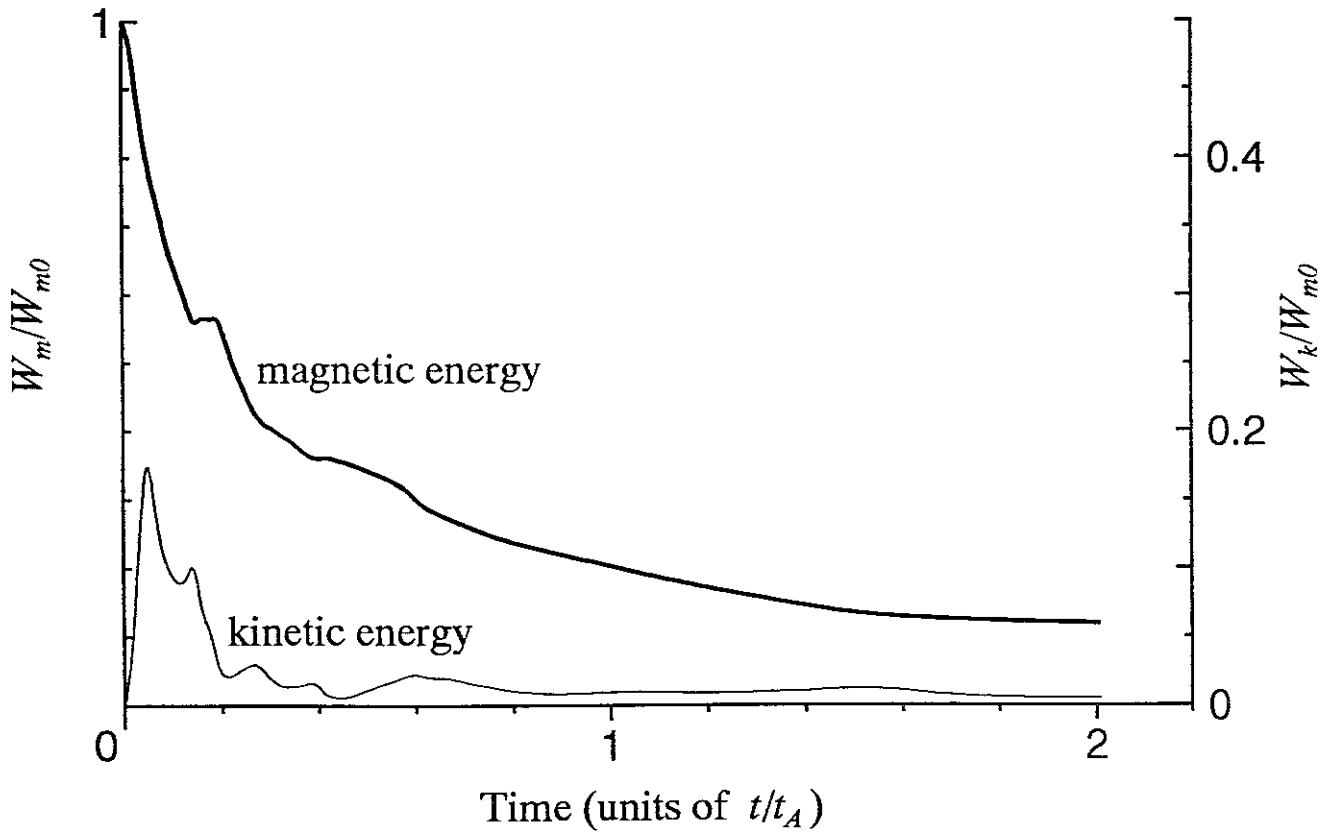
1
0
1
2
0.4
0.2
0
W_m/W_{m0}
W_k/W_{m0}
magnetic energy
kinetic energy
Time (units of t/t_A)

Fig.5

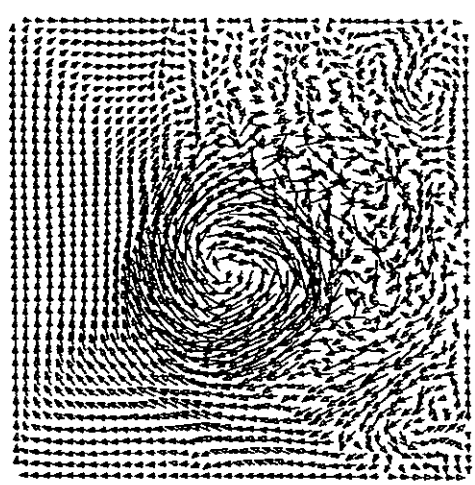

Fig.6

Recent Issues of NIFS Series

NIFS-376 S. Bazdenkov, T Sato, K. Watanabe and The Complexity Simulation Group,
Multi-Scale Semi-Ideal Magnetohydrodynamics of a Tokamak Plasma; Sep. 1995

NIFS-377 J. Uramoto,
Extraction of Negative Pionlike Particles from a H2 or D2 Gas Discharge Plasma in Magnetic Field; Sep. 1995

NIFS-378 K. Akaishi,
Theoretical Consideration for the Outgassing Characteristics of an Unbaked Vacuum System; Oct. 1995

NIFS-379 H. Shimazu, S. Machida and M. Tanaka,
Macro-Particle Simulation of Collisionless Parallel Shocks; Oct. 1995

NIFS-380 N. Kondo and Y. Kondoh,
Eigenfunction Spectrum Analysis for Self-organization in Dissipative Solitons; Oct. 1995

NIFS-381 Y. Kondoh, M. Yoshizawa, A. Nakano and T. Yabe,
Self-organization of Two-dimensional Incompressible Viscous Flow in a Friction-free Box; Oct. 1995

NIFS-382 Y.N. Nejoh and H. Sanuki,
The Effects of the Beam and Ion Temperatures on Ion-Acoustic Waves in an Electron Beam-Plasma System; Oct. 1995

NIFS-383 K. Ichiguchi, O. Motojima, K. Yamazaki, N. Nakajima and M. Okamoto
Flexibility of LHD Configuration with Multi-Layer Helical Coils; Nov. 1995

NIFS-384 D. Biskamp, E. Schwarz and J.F. Drake,
Two-dimensional Electron Magnetohydrodynamic Turbulence; Nov. 1995

NIFS-385 H. Kitabata, T. Hayashi, T. Sato and Complexity Simulation Group,
Impulsive Nature in Collisional Driven Reconnection; Nov. 1995

NIFS-386 Y. Katoh, T. Muroga, A. Kohyama, R.E. Stoller, C. Namba and O. Motojima,
Rate Theory Modeling of Defect Evolution under Cascade Damage Conditions:The Influence of Vacancy-type Cascade Remnants and Application to the Defect Production Chracterization by Microstructural Analysis; Nov. 1995

NIFS-387 K. Araki, S. Yanase and J. Mizushima,
Symmetry Breaking by Differential Rotation and Saddle-node Bifurcation of the Thermal Convection in a Spherical Shell; Dec. 1995

NIFS-388 V.D. Pustovitov,
Control of Pfirsch-Schlüter Current by External Poloidal Magnetic Field in Conventional Stellarators: Dec. 1995

NIFS-389 K. Akaishi,
On the Outgassing Rate Versus Time Characteristics in the Pump-down of an Unbaked Vacuum System; Dec. 1995

NIFS-390 K.N. Sato, S. Murakami, N. Nakajima, K. Itoh,
Possibility of Simulation Experiments for Fast Particle Physics in Large Helical Device (LHD); Dec. 1995

NIFS-391 W.X.Wang, M. Okamoto, N. Nakajima, S. Murakami and N. Ohyabu,
A Monte Carlo Simulation Model for the Steady-State Plasma in the Scrape-off Layer; Dec. 1995

NIFS-392 Shao-ping Zhu, R. Horiuchi, T. Sato and The Complexity Simulation Group,
Self-organization Process of a Magnetohydrodynamic Plasma in the Presence of Thermal Conduction; Dec. 1995

NIFS-393 M. Ozaki, T. Sato, R. Horiuchi and the Complexity Simulation Group
Electromagnetic Instability and Anomalous Resistivity in a Magnetic Neutral Sheet; Dec. 1995

NIFS-394 K. Itoh, S.-I Itoh, M. Yagi and A. Fukuyama,
Subcritical Excitation of Plasma Turbulence; Jan. 1996

NIFS-395 H. Sugama and M. Okamoto, W. Horton and M. Wakatani,
Transport Processes and Entropy Production in Toroidal Plasmas with Gyrokinetic Eletromagnetic Turbulence: Jan. 1996

NIFS-396 T. Kato, T. Fujiwara and Y. Hanaoka,
X-ray Spectral Analysis of Yohkoh BCS Data on Sep. 6 1992 Flares - Blue Shift Component and Ion Abundances -; Feb. 1996

NIFS-397 H. Kuramoto, N. Hiraki, S. Moriyama, K. Toi, K. Sato, K. Narihara, A. Ejiri, T. Seki and JIPP T-IIU Group,
Measurement of the Poloidal Magnetic Field Profile with High Time Resolution Zeeman Polarimeter in the JIPP T-IIU Tokamak; Feb. 1996

NIFS-398 J.F. Wang, T. Amano, Y. Ogawa, N. Inoue,
Simulation of Burning Plasma Dynamics in ITER; Feb. 1996

NIFS-399 K. Itoh, S-I. Itoh, A. Fukuyama and M. Yagi,
Theory of Self-Sustained Turbulence in Confined Plasmas; Feb. 1996

NIFS-400 J. Uramoto,
A Detection Method of Negative Pionlike Particles from a H2 Gas

Descharge Plasma; Feb. 1996

NIFS-401 K.Ida, J.Xu, K.N.Sato, H.Sakakita and JIPP TII-U group,
Fast Charge Exchange Spectroscopy Using a Fabry-Perot Spectrometer in the JIPP TII-U Tokamak; Feb. 1996

NIFS-402 T. Amano,
Passive Shut-Down of ITER Plasma by Be Evaporation; Feb. 1996

NIFS-403 K. Orito,
A New Variable Transformation Technique for the Nonlinear Drift Vortex; Feb. 1996

NIFS-404 T. Oike, K. Kitachi, S. Ohdachi, K. Toi, S. Sakakibara, S. Morita, T. Morisaki, H. Suzuki, S. Okamura, K. Matsuoka and CHS group; *Measurement of Magnetic Field Fluctuations near Plasma Edge with Movable Magnetic Probe Array in the CHS Heliotron/Torsatron*; Mar. 1996

NIFS-405 S.K. Guharay, K. Tsumori, M. Hamabe, Y. Takeiri, O. Kaneko, T. Kuroda,
Simple Emittance Measurement of H- Beams from a Large Plasma Source; Mar. 1996

NIFS-406 M. Tanaka and D. Biskamp,
Symmetry-Breaking due to Parallel Electron Motion and Resultant Scaling in Collisionless Magnetic Reconnection; Mar. 1996

NIFS-407 K. Kitachi, T. Oike, S. Ohdachi, K. Toi, R. Akiyama, A. Ejiri, Y. Hamada, H.Kuramoto, K. Narihara, T. Seki and JIPP T-IIU Group,
Measurement of Magnetic Field Fluctuations within Last Closed Flux Surface with Movable Magnetic Probe Array in the JIPP T-IIU Tokamak; Mar. 1996

NIFS-408 K. Hirose, S. Saito and Yoshi.H. Ichikawa
Structure of Period-2 Step-1 Accelerator Island in Area Preserving Maps; Mar. 1996

NIFS-409 G.Y.Yu, M. Okamoto, H. Sanuki, T. Amano,
Effect of Plasma Inertia on Vertical Displacement Instability in Tokamaks; Mar. 1996

NIFS-410 T. Yamagishi,
Solution of Initial Value Problem of Gyro-Kinetic Equation; Mar. 1996

NIFS-411 K. Ida and N. Nakajima,
Comparison of Parallel Viscosity with Neoclassical Theory; Apr. 1996

NIFS-412 T. Ohkawa and H. Ohkawa,
Cuspher. A Combined Confinement System; Apr. 1996

NIFS-413 Y. Nomura, Y.H. Ichikawa and A.T. Filippov,
Stochasticity in the Josephson Map; Apr. 1996

NIFS-414 J. Uramoto,
Production Mechanism of Negative Pionlike Particles in H_2 Gas Discharge Plasma; Apr. 1996

NIFS-415 A. Fujisawa, H. Iguchi, S. Lee, T.P. Crowley, Y. Hamada, S. Hidekuma, M. Kojima,
Active Trajectory Control for a Heavy Ion Beam Probe on the Compact Helical System; May 1996

NIFS-416 M. Iwase, K. Ohkubo, S. Kubo and H. Idei
Band Rejection Filter for Measurement of Electron Cyclotron Emission during Electron Cyclotron Heating; May 1996

NIFS-417 T. Yabe, H. Daido,T. Aoki, E. Matsunaga and K. Arisawa,
Anomalous Crater Formation in Pulsed-Laser-Illuminated Aluminum Slab and Debris Distribution; May 1996

NIFS-418 J. Uramoto,
Extraction of K^- Mesonlike Particles from a D_2 Gas Discharge Plasma in Magnetic Field; May 1996

NIFS-419 J. Xu, K. Toi, H. Kuramoto, A. Nishizawa, J. Fujita, A. Ejiri, K. Narihara, T. Seki, H. Sakakita, K. Kawahata, K. Ida, K. Adachi, R. Akiyama, Y. Hamada, S. Hirokura, Y. Kawasumi, M. Kojima, I. Nomura, S. Ohdachi, K.N. Sato
Measurement of Internal Magnetic Field with Motional Stark Polarimetry in Current Ramp-Up Experiments of JIPP T-IIU; June 1996

NIFS-420 Y.N. Nejoh,
Arbitrary Amplitude Ion-acoustic Waves in a Relativistic Electron-beam Plasma System; July 1996

NIFS-421 K. Kondo, K. Ida, C. Christou, V.Yu.Sergeev, K.V.Khlopenkov, S.Sudo, F. Sano, H. Zushi, T. Mizuuchi, S. Besshou, H. Okada, K. Nagasaki, K. Sakamoto, Y. Kurimoto, H. Funaba, T. Hamada, T. Kinoshita, S. Kado, Y. Kanda, T. Okamoto, M. Wakatani and T. Obiki,
Behavior of Pellet Injected Li Ions into Heliotron E Plasmas; July 1996

NIFS-422 Y. Kondoh, M. Yamaguchi and K. Yokozuka,
Simulations of Toroidal Current Drive without External Magnetic Helicity Injection; July 1996